Effects of Non-Idealities on Gain in a Detonation Cycle

Riley Huff and Mirko Gamba
University of Michigan
Ann Arbor, MI, United States of America

1 Introduction

Rotating Detonation Engines (RDEs) have received increased development interest in the recent decades because of the drive for the aerospace community to move to more efficient power generation and propulsion solutions. By harnessing the products of a continually propagating detonation wave, a RDE theoretically achieves a pressure gain across the wave, leading to a theoretical improved efficiency in energy conversion due to a reduction of the entropy generated during the combustion process.

However, one of the key challenges is assessing and demonstrating the degree of improved combustion performance that can be achieved, in practice, over conventional deflagration-based devices. Several past studies have considered different approaches to assess this aspect. Typically, theoretical evaluations consider a comparison between representations of the RDE cycle using an average thermodynamic state analysis of the cycle's temperature-entropy ($T-s$) diagram [1, 2, 3]. Cycle analysis using $T-s$ diagrams is typically conducted using either an ideal representation of the detonation cycle, or by using CFD results. The ideal cycle analysis is limited by the unrealistic idealization, while the use of CFD is limited by the underlying CFD models and assumptions used in the computations. Experimentally, measured thrust is used as a surrogate to quantify the available work at the RDE exit, relative to a deflagration at the same conditions, through the concept of Equivalent Available Pressure (EAP) proposed by Kaemming and Paxson [4]. However, the the accuracy EAP method is limited by measurement accuracy and the validity in its underlying assumptions.

The present study proposes an alternative approach combining the two traditional approaches by using certain measured quantities (e.g., pressure ratio across the detonation wave) while estimating certain loss quantities (e.g., fraction of parasitic combustion) in functioning RDEs to inform a cycle $T-s$ diagram with additional intermediate states associated with different loss mechanism. The study relies on an extension of the deflagration loss model proposed by Huff and Gamba, to estimate deflagration losses in a RDE using measured detonation wave performance values [5]. The goal of the proposed model is therefore to expand the traditional RDE cycle analysis to generate measures of overall RDE cycle performance that accounts for losses and produces observed experimental trends of RDE performance.

2 Model Description and Methodology

To facilitate the description of the proposed model, a review key properties of the description of a detonation wave is needed. Chapman-Jouguet (CJ) theory provides a 1-D steady state control volume

Correspondence to: ryhuff@umich.edu

analysis of the detonation process in the reference frame of the detonation wave: beginning with fresh reactants at a give initial state, which are converted to the post combustion state at the CJ plane. One might assume that the CJ state is the state from which work may be extracted; however, this view would be incomplete and would result in estimating an available energy higher than the energy released from combustion. Early research on detonation waves in ducts has shown that the detonation wave is accompanied by a Taylor expansion wave the emanates from the CJ plane to properly match the boundary conditions at the far-end from the wave of a given system [6, 7]. This process is shown for an ideal detonation tube with a fixed end-wall boundary condition on the left in Figure 1(a). In this figure, state ③ represents the reactants ahead of the detonation wave, state ③.② represents the CJ plane, and state ④ is state at the tail of the expansion wave that enforces the flow velocity to the end-wall velocity boundary condition in the laboratory frame of reference (i.e., $u_{4_{\mathrm{Det}}} = u_{\mathrm{w}} = 0$). To be complete, state ③.① is known as the von-Neumann condition, or the location of fresh reactants that have been processed by the leading shock wave, but have yet to begin chemical reaction. The post-expansion state, state ④, is now recognized as the state from which work may be extracted. However, with a fixed boundary, the tail of the expansion wave is moving at a lower velocity relative to the detonation wave, resulting in a growing expansion wave region. This means that even in the wave reference frame, the process is unsteady, and the same steady control volume analysis conducted in CJ theory cannot be applied. Rather, the final state ④ can be evaluated by matching the CJ solution across the detonation wave and the method of characteristic solution of an isentropic unsteady expansion wave to the end-wall velocity condition.

This study seeks to model RDEs instead, which have a different far-end boundary condition for the detonation wave system that results in a much simpler analysis. Figure 1(b) shows a 1-D simplified representation of the wave system within a RDE, where the next wave, more specifically the state ahead of the next wave, acts as a far-end boundary moving with the same speed as the wave system. This treatment of the RDE cycle implies that the expansion wave remains of fixed width and stationary as observed in the frame of reference of the detonation wave, allowing for a steady state analysis of the complete wave system (detonation and expansion waves combined) in the detonation wave frame of reference. The question remains as to how this expansion process should be modeled, and why it is important to capture this process in a state-resolved analysis. By expanding from the CJ plane, energy is returned to the system in proportion to the energy of the moving reference frame. The magnitude of this energy can be calculated through the coordinate transform of the energy equation from the wave frame to the laboratory frame, a process explained in detail by Nordeen *et al.* [2, 3]. This coordinate transform results in the conservation of rothalpy equation, shown by Equation 1 for the conservation from the reactants, state ③ to the CJ plane, state ③.②:

$$h_3 + \frac{u_3^2}{2} - Du_3 + q = h_{3.2} + \frac{u_{3.2}^2}{2} - Du_{3.2} \tag{1}$$

where, u_i is the velocity of the gas at state ⓘ in the laboratory frame of reference and q is the specific heat added across the wave. The term Du_i accounts for the energy required to move the wave reference frame. To determine the final state, state ④ the conservation of rothalpy equation is applied between the CJ plane, state ③.② and the post expansion state, state ④ in Equation 2:

$$h_{3.2} + \frac{u_{3.2}^2}{2} - Du_{3.2} = h_4 + \frac{u_4^2}{2} - Du_4. \tag{2}$$

Combining Equation 1 and Equation 2 and assuming u_3 and u_4 are zero, this equation set reduces to:

$$c_{p,3}T_3 + q = c_{p,4}T_4 \tag{3}$$

which is a familiar form of the energy conservation equation of a steady combustion process in the laboratory frame. With this formulation, the energy of the complete system, which is defined as one rotational cycle of the detonation wave, is properly accounted and the available energy remains bounded by the heat release of the reacting mixture.

To examine the non-ideal effects on a detonation wave, this model is extended to include three additional loss mechanisms: inlet pressure losses, parasitic deflagrative combustion ahead of the main detonation wave, and unburnt fuel passing through the detonation, without contributing to the heat release process in the detonation wave. The pressure loss term can be thought of as a total pressure loss across an arbitrary inlet system, or the static to total pressure change that occurs in an RDE inlet as the area expands into the channel. Since the combustion process and detonation wave depend only on the static pressure at which they occur, these two representations of inlet pressure losses are essentially the same with respect to the results of this model. This simplification allows the analysis to be extended to a 2-D system under certain assumptions and restrictions. The other two loss mechanisms, and their effects on the detonation wave performance, were discussed in detail by Huff and Gamba [5], so they are not repeated here for brevity.

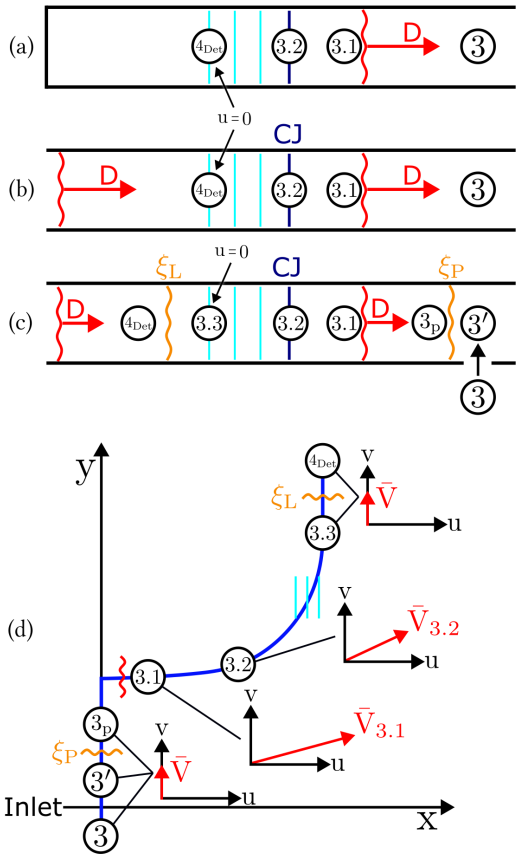

Figure 1: State diagram for multiple detonation based systems. Ideal detonation tube (a). Ideal RDE (b). Non-ideal RDE (c). Example particle path for a non-ideal RDE (d).

Figure 1(c) shows the station used in the analysis for the non-ideal wave, where state ③ is the reactant mixture before injection, ③′ is the post injection state after any pressure losses, $③_p$ is the state after any parasitic combustion, ③.③ represent the frozen chemistry post expansion state from the CJ plane, state ③.②, before any additional combustion from leaked fuel, and now $④_{Det}$ is the final state after commensal combustion of the leaked fuel. This final state is modeled as the equilibrium composition at the post expansion pressure, which assumes complete combustion post-expansion.

The methodology of modeling a 3-D RDE flow-path with a 1-D state-to-state representation is shown in Figure 1(d), with a representative particle path of the model shown in blue. It should be noted that this diagram is representing a particle path in the lab frame of reference. Assuming no radial variation reduces the problem to 2-D, where the axial flow direction is denoted as the y direction and the aziumathal component, in the direction of the detonation wave propagation, is denoted as the x direction. Next, assuming the axial component of velocity, v, is constant from state ③′ to $④_{Det}$ allows the states to be modeled in a 1-D setting. While this assumption is not perfectly valid, as the velocity would increase on average as the combustion process proceeds, the same treatment was applied to the ideal deflagration case, where no velocity change is accounted. The velocity diagrams in Figure 1(d) provide more insight into these assumptions, where the shock wave imparts an azimuthal velocity, $u_{3.1}$, to the flow. In accordance with ZND theory, as the combustion occurs towards the CJ plane, the magnitude of the velocity decreases. One final assumption of the model is that the zero azimuthal velocity input from state ③ acts as the boundary condition for the proceeding wave, meaning that the expansion process

from the CJ plane, state (3.2), to the post-expansion state, state (3.3), reduces the azimuthal velocity, $u_{3.3}$, back down to zero.

Finally, to compare the results of this model to an ideal deflagration device, it is necessary to determine the amount of work available to extract. This was done by calculating the specific thrust production from each respective final state, state (4), if isentropically expanded to atmospheric conditions, 1 atm in the case of this study. This was done by adapting the method discussed by Shepherd and Kasahara [8] to the present formulation according to:

$$u_e = \sqrt{h_4 - h(P, s_4)}. \tag{4}$$

where u_e represents the stream thrust velocity after an isentropic expansion to ambient conditions, or simply the specific thrust. This can easily be converted to an ideal thrust estimate F according to $F = \dot{m} u_e$. With a proper metric of comparison established, the results of this model can now be examined.

3 Results

The hierarchy of models presented in this study were evaluated with the use of the *Cantera* package for *Python* [9], and included the deflagration loss model from Huff and Gamba [5]. The state properties at the relevant states defined in the model were evaluated, with particular focus on state (4) conditions.

Figure 2(a) shows an example $T - s$ diagram for an ideal detonation at a given set of initial pressure, temperature and equivalence ratio. It is important to note that this plot is comparing total temperatures on the y-axis, where the assumed velocity of the detonation states follow Figure 1(d) and the deflagration velocity is assumed zero. The results are shown for a hydrogen air detonation at an equivalence ratio of 0.6, and without any deflagration losses. The states and processes in Figure 2 are in accordance to the description given in Section 2.

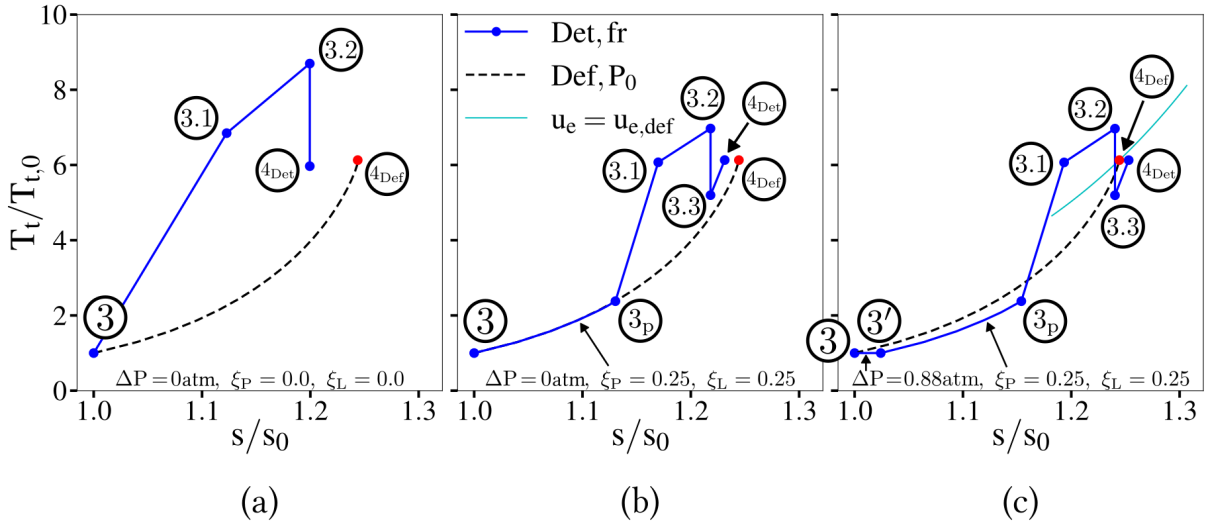

Figure 2: T-s diagrams for RDE cycles: Ideal RDE cycle (a). RDE cycle with deflagration losses (b). RDE cycle with deflagration and inlet losses (c). Initial Conditions: $H_2 - Air$, $\phi = 0.6$, $P_0 = 2.14$ atm, $T_0 = 294$ K

Figure 2(a) shows the relationship between the final state of each process, and shows a similar results seen in Dyer *et al.* where the detonation is at a similar final temperature, but at much lower entropy

production [1]. This results in a theoretically higher post combustion pressure, showing pressure gain over the deflagration cycle, allowing for more work extraction if expanding to the same final pressure. When extending this model to capture deflagration losses, Figure 2(b), was constructed at the same initial conditions for Figure 2(a) but now with parasitic and leaked fractions of $\zeta_P = \zeta_L = 0.25$ (see [5]). This plot now shows the parasitic combustion ahead of the wave following the line of constant pressure combustion as expected, state ③ to state (3_p). Because of the change in properties ahead of the wave, and the fact that not all of the remaining fuel is contributing to the detonation heat release, there is a noticeably weaker shock moving from state (3_p) to state (3.1). This was discussed in detail in prior work and leads to the conclusion that parasitic combustion ahead of the detonation wave has the most drastic reduction in detonation wave performance [5]. Next, the fraction of fuel that is consumed by the detonation combusts, moving to state (3.2). A similar frozen expansion wave moves the process to state (3.3) accounting for the lower, but still significant, $Du_{3.2}$ energy term. Finally, an assumption of equilibrium combustion, at the post expansion pressure, of the remaining fuel moves the process to state (4_{Det}). Accounting for deflagration losses, this final state is much closer to the a deflagration occurring at the same initial conditions. It should be noted that these estimates of deflagration fractions are on the lower end of the spectrum of values found in Huff and Gamba [5].

The $T - s$ diagrams in Figures 2(a) and 2(b) can be extended to include the effects of pressure losses through an inlet, a measured quantity of interest used to inform this model. Figure 2(c) shows the non-ideal detonation states, with the same deflagration loss fractions as Figure 2(b), but now with a 0.88 atm pressure drop from state ③ to (3′). The pressure loss value used in this example corresponds to the channel static pressure to plenum total pressure change for a particular experimental run, around which all of the initial conditions and deflagration loss fractions were determined. The parasitic combustion ahead of the detonation occurs at this reduced pressure, which is seen below the dashed black line of constant pressure deflagration at the plenum pressure. With the addition of the pressure loss term, the post expansion state, (3.3), falls at a similar entropy production as the deflagration final state, (4_{Def}), but at a much lower temperature and pressure. If state (3.3) equilibrates at the post expansion pressure, then the final state from which work can be extracted, (4_{Det}), produced more entropy than the deflagration at the initial conditions at a similar temperature.

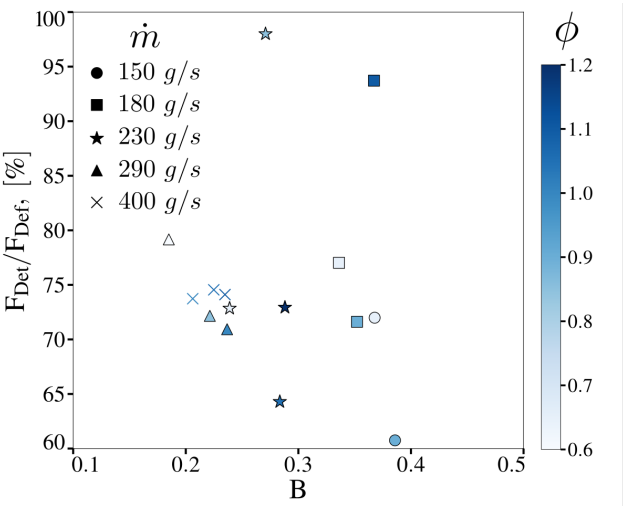

Figure 3: Thrust as a fraction of ideal deflagration thrust versus inlet blockage.

Using the adapted specific thrust formulation in Equation 4, a line of constant specific thrust can be calculated at the deflagration final state, (4_{Def}), shown by the cyan solid line through state (4_{Def}). Any final state above this line produces more thrust than the ideal deflagration process, and any point below correspond to less efficient thrust production. Now that the line of constant specific thrust has been established, the reader can return to Figure 2(c) and notice that the final state for the detonation cycle, (4_{Det}), is below the line of constant specific thrust, showing the detonation cycle produces less thrust than the ideal deflagration. For reference, the post detonation state results in a final pressure of 1.70 atm versus the 2.11 atm initial condition, which is more in line with experimental channel pressure measurements at the exit of the RDE channel.

With the estimated nozzle exit velocity, assuming perfectly expanded flow, and the known mass flow rate for a given set of data, the predicted thrust can be calculated for both the modeled detonation cycle and an ideal deflagration. Figure 3 shows the the predicted thrust for the modeled RDE as a percentage of the ideal deflagration thrust. This performance metric is plotted against the calculated inlet blockage, similar to the analysis conducted by Huff and Gamba [5], where lower values of blockage correlate to a much stiffer injection system. Across this set of runs, the predict thrust of the RDE consistently underperformed the ideal deflagration thrust production, a trend echoed by experimental thrust measurements.

4 Conclusion

The goal of this study was to establish a realistic state-to-state model of a RDE device capable of including loss mechanisms, allowing for the comparison to a deflagration system operating at the same initial conditions. The initial results of the model suggests that the combination of reduced static pressure and parasitic deflagration combustion ahead of the wave results in a drastic reduction in RDE thrust generation, relative to an ideal RDE cycle. At experimental values for static channel pressure and the associated parasitic combustion fraction, no case analyzed in this study had an estimated thrust above the ideal deflagration cycle with the same initial conditions, something routinely seen in experiments. These results suggest that a lower inlet pressure loss, or reduced fill velocity, would be the main areas of improvement to increase thrust performance. However, these results run counter to the results of Huff and Gamba [5], where a stiffer inlet system helped to reduce the parasitic combustion fraction. Unfortunately, a stiffer inlet inherently requires a larger inlet pressure ratio, leading to an inverse relationship between the two most impactful loss terms.

References

[1] R. Dyer and T. Kaemming. “The Thermodynamic Basis of Pulsed Detonation Engine Thrust Production”. In: *38th AIAA/ASME/SAE/ASEE Joint Propulsion Conference*. AIAA, July 2002.

[2] C. Nordeen et al. “Energy Transfer in a Rotating Detonation Engine”. In: *47th AIAA/ASME/SAE/ASEE Joint Propulsion Conference & Exhibit*. 2011, p. 6045.

[3] C. A. Nordeen and D. A. Schwer. “Quasi-steady-state Analysis of a High Resolution Detonation Simulation”. In: *AIAA Scitech 2019 Forum*. 2019, p. 1745.

[4] T. A. Kaemming and D. E. Paxson. “Determining the Pressure Gain of Pressure Gain Combustion”. In: *2018 Joint Propulsion Conference*. Paper No. AIAA-2018-4567, 2018.

[5] R. Huff and M. Gamba. “Markov Chain Monte Carlo Parameter Estimation of Deflagration Losses in a Rotating Detonation Engine”. In: *AIAA SCITECH 2023 Forum*. Paper No. AIAA-2023-1293.

[6] H. Langweiler. *The Hydrodynamic Theory of Detonation*. Tech. rep. 1939.

[7] G. I. Taylor. “The Dynamics of the Combustion Products Behind Plane and Spherical Detonation Fronts in Explosives”. In: *Proceedings of the Royal Society of London. Series A. Mathematical and Physical Sciences* 200.1061 (1950), pp. 235–247.

[8] J. E. Shepherd and J. Kasahara. “Analytical Models for the Thrust of a Rotating Detonation Engine”. In: *Technical Report FM2017.001* (2017).

[9] D. G. Goodwin et al. “Cantera: An Object-oriented Software Toolkit for Chemical Kinetics, Thermodynamics, and Transport Processes”. In: (2021). Version 2.5.1.